

Supplementary Methods

Cell transportation

To measure cell stiffness, cells were transported from New York University in Tuxedo, New York to Duke University in Durham, North Carolina. All cell lines were transported live with the exception of the A549 cells, the Arsenic 4w cells and the BEAS-2B control cells, which were transported frozen via overnight shipping. All other cell lines were transported in 25 cm² flasks that were cultured to confluence and filled to capacity with media. Cells were transported for approximately 12 hours at which point excess media was removed and cells were returned to the normal culture conditions in the incubator at Duke.

G1 selection protocol

Cells were visually selected in order to constrain the cell cycle phase sampled during imaging. Supplementary figure S1 contains images in a range of cell cycle phases to illustrate those that were selected during measurement and those that were avoided during measurement. Later stage (G2) phases were avoided due to the highly spread morphology (Supplementary figure S1, Panels J-L), and presented with less dense regions than the G1 phase (Supplementary figure S1, Panels A-C). Cells that were dividing or mitotic were poorly attached and were easily detectable during measurement because they moved in the transverse direction with application of shear force (Supplementary figure S1, Panels D-E) or could be observed dividing (Supplementary figure S1, Panels F-I). Cells that were clustered or touching other cells were avoided during sampling because it would not be possible to extract accurate information using the refocus algorithm or Kelvin-Voigt model (Supplementary figure S-1, Panel L).

Post-measurement G1 data filtration

The visual selection protocol to restrict sampling to cells in the G1 phase was accompanied by a data filtration step to insure that no G2 or dividing cells were inadvertently sampled. To check for

this occurrence, mean surface area was computed for each treatment group, and the cells with surface areas that were more than three standard deviations larger than the group mean surface area were flagged for further analysis. The flagged cells were visually evaluated to determine whether the cells were in G2 or splitting. G2 cells exhibited a more spread morphology with multiple cellular projections. Splitting cells appeared to have a dip in their phase profile at the cell splitting junction. G1 cells appeared less spread and more dense, with a prototypical tear drop shape. These post-processing checks provided an additional measure to confirm proper cell selection occurred during sampling.

Image processing

Image processing was performed in MATLAB version R2013a (Mathworks, Natick MA) and is described in the supplement. Phase data were extracted using custom MATLAB code that has been previously described [1]. The image was digitally refocused to determine the true focal plane, using a previously established refocusing algorithm [2] and after cells were masked individually to ensure proper refocusing around the region of interest. Following refocusing, the phase profile was unwrapped to remove 2π ambiguities, and the background phase field was fit with a low order polynomial and subtracted to reveal the detrended cellular phase image. This phase profile allowed for the generation of a quasi-3D cellular image via the assumption of a homogenous refractive index difference ($\Delta n = 0.02$) [3]. From the phase information, the optical path length (OPL), defined as $OPL = \varphi(x, y)\lambda / (2\pi)$ at each pixel within the cell was recorded. Examples of the cell images are presented in Figures 2B and 2C and also in Supplementary Figure S1.

Image sets were filtered in order to remove any errors generated from the image processing algorithms by rejecting image sets where the COM displacement measurements were corrupted by noise. To generate this filter, signal to noise ratios (SNR) were calculated for the COM shift for each imaged cell. SNR was calculated as the ratio of the steady state COM displacement to the standard deviation of the COM variation during the static portion of the

imaging. Any cells exhibiting a COM shift with an SNR less than 10 were removed from the dataset.

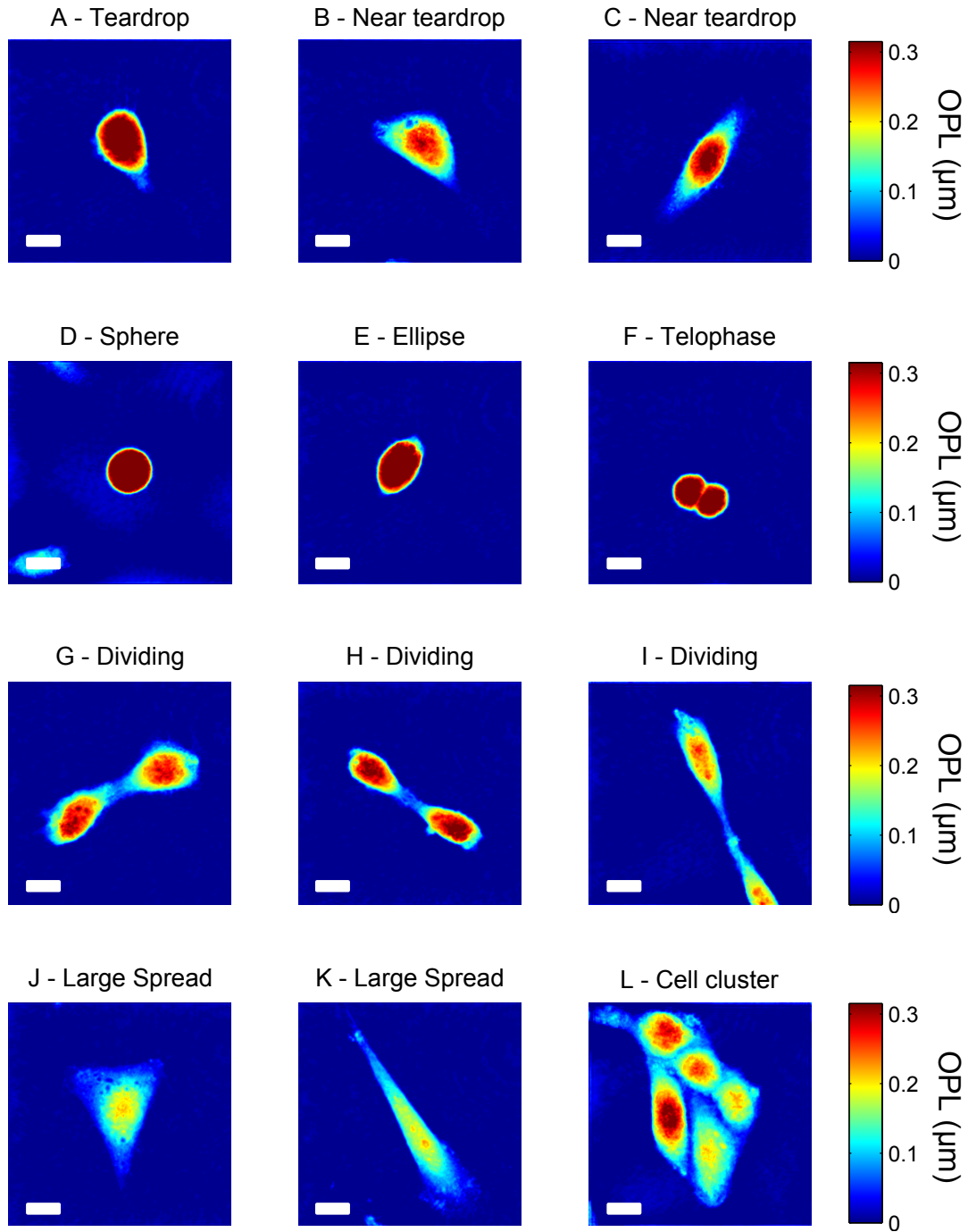
Supplementary Table I. Back-transformed model estimates of treatment and orientation effects with 95% confidence intervals. The back-transformed treatment estimates represent population medians of effective shear stiffness for orientation zero. The values are illustrated in Figure 3D (Arsenic 4w, Arsenic 12w, BEAS-2B) and Figure 4F (Arsenic clones, BEAS-2B clones).

	Estimate	CI Lower	CI Upper
Arsenic 4w	2.28	1.87	2.77
Arsenic 12w	1.90	1.61	2.23
BEAS-2B	3.05	2.56	3.64
Arsenic clones	1.84	1.73	1.95
BEAS-2B clones	2.58	2.38	2.81
Orientation	1.0012	1.0003	1.0020

Supplementary Table II. Model-based estimates of within-group RSD of cellular shear stiffness

Treatment group	RSD
Arsenic 4w	0.83
Arsenic 12w	0.79
BEAS-2B	0.84
Arsenic clones	0.55
BEAS-2B clones	0.71

Supplementary Fig S1. Visual selection protocol optical path length image examples. Optical path length images of cells prior to application of shear flow. Images provide a range of examples of cells that were or were not selected for stiffness assessment. Images A-C represent cells in the G1 phase of the cell cycle and are representative of cells selected for assessment with shear flow. Images D-L are examples of cells that were avoided for assessment with shear flow. Image A exhibits the optimal teardrop shape of cells in early G1. Images B-C are exhibit near tear-drop shapes of later G1. Images D-E are examples of cells in mitosis which assume spherical shapes and lose connection to substrate. Images F-I are examples of cells in later stages of mitosis where two cellular bodies are evident. Images J-L are examples of cells that are in S or G2 exhibiting more developed and spread morphologies which occur in later stages of the cell cycle for BEAS-2B cells. Scale bars represent 10 microns.



References

1. Rinehart, M., *et al.* (2012) Quantitative phase spectroscopy. *Biomed. Opt. Express*, **3**, 958-965.
2. Rinehart, M.T., *et al.* (2015) Influence of defocus on quantitative analysis of microscopic objects and individual cells with digital holography. *Biomed. Opt. Express*, **6**, 2067-2075.
3. Eldridge, W.J., *et al.* (2016) Imaging deformation of adherent cells due to shear stress using quantitative phase imaging. *Opt. Lett.*, **41**, 352-355.